

DESIGN AND PRODUCTION OF A FREE-FORM LENS FOR LONG RANGE LED ILLUMINATION

AHMET BINGÜL, MEHMET ADIYAMAN

Department of Engineering of Physics, Gaziantep University, Gaziantep 27310, Turkey.

In this study, a procedure for designing a free-form lens for long-range LED illumination is presented. The geometrical form of the proposed lens is obtained by minimizing optical path lengths of the rays emitted from a point-like light source. Optical ray tracing simulations of two different LEDs and the free-form lens are performed by using Zemax OpticStudio. In addition, the prototype of the free-form lens is manufactured by the plastic injection molding method using PMMA material. Nine of the lenses are used to build an LED projector in the form of a 3x3 lens matrix. The optical measurements of the projector are compared with the results predicted in the simulations. It is found that the beam divergence of the projector is less than 10 degrees when using suitable LEDs in visible and near infrared regions.

1. Introduction

LED (Light Emitting Diode) is an energy-saving source providing high light efficiency and has a long life time. Despite the high light efficiency, in general, the direct light output of LEDs spread at wide angle. This results in a disadvantage in the use of LEDs when illuminating a surface being at a large distance from the source. The light intensity on a target can be improved either by using reflectors or by placing the narrow-angle free-form lenses having a suitable geometry in front of the LEDs.

There are many academic and engineering studies on design and production of free-form lenses in literature such as [1, 2, 3, 4, 5, 6]. These studies are mostly based on defining a differential equation related to design and its numerical solution to obtain the geometrical form of the lens. In this study, however, a free-form lens design based on optical path length calculations is presented for long-range (or narrow-angle) illumination for both near infrared (IR) and visible regions. Optical ray tracing analyses of LEDs and the free-form lens are developed in Zemax OpticStudio 20.1 [7]. Three different

polymers are used as lens materials; PMMA (poly(methyl methacrylate)), PC (polycarbonate) and PS (polystyrene). Simulation studies show that PMMA exhibits a better performance in terms of total optical power on the detector compared to others.

In addition, the prototype of solid form of the lens made from PMMA is manufactured via plastic injection molding method. Nine of them are used to build a projector which is basically a 3x3 lens array. By using two different LEDs (white and IR), optical measurements of the projector are compared with the predictions of Zemax. Results seem to be consistent with that of simulations and the beam divergence of the projector for visible and IR regions are found to be less than 10° .

2. Free-Form Lens Profile

Free-form lenses are preferred in both illumination [2, 6] and imaging systems [3]. In this study, a profile of a free-form lens to be used in LED illumination is proposed in order to obtain a narrow-angle beam spot at long distances.

The free-form lens (or simply referred to as lens) is assumed to be used in air and has index of refraction n . For simplicity, one can start the design with a point-like source placed at the origin of x-y coordinate system and with one-dimensional curves representing the *surfaces* of the lens. Aim of the lens is to deflect all of the rays emitted from the source such that they are parallel to optical axis on the exit side of the lens. Figure 1 shows the selected curves and four rays originating from the point source placed at origin. Shape of the surface 1 and 2 are non-linear functions. The remaining surfaces are represented by lines. Therefore, there are four design parameters which affect the optical performance and geometrical size of the lens; the lengths p , q , h and refractive index n .

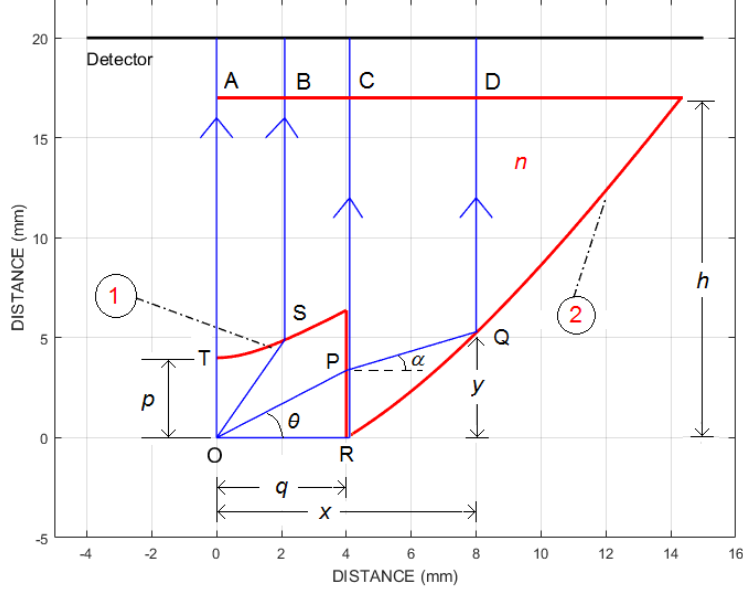


Fig. 1. Surfaces of free-form lens and rays used in the analysis.

The shape of the first surface can be found as follows. We desire that the optical path lengths (OPL)¹ for rays A and B must be equal so that they reach the detector (or target) at the same time, namely, $OPL_A = OPL_B$ where $OPL_A = |OT| + n|TA|$ and $OPL_B = |OS| + n|SB|$. By substituting the lengths we obtain

$$p + n(h - p) = \sqrt{x^2 + y^2} + n(h - y) \quad (1)$$

where p is the shortest distance between origin and surface 1, and $x \leq q$. Solving for y yields two roots:

$$y(x) = \frac{np}{n+1} \pm \sqrt{\left(\frac{x}{n-1}\right)^2 + \left(\frac{p}{n+1}\right)^2} \quad (2)$$

This is a well-known curve called the hyperbola whose focus is at the origin. Positive root, $y(x) > 0$, is used in the analysis.

Surface 2 is slightly complicated since ray C and D will be first refracted on the plane at point R and P respectively. Then, they are totally reflected at point R and Q. Again, we desire their optical paths must be the same

¹ OPL is defined as the product of the refractive index of the medium and geometrical path traversed by a ray. Time of flight for the ray in the medium is given by $t = OPL/c$ where c is the speed of light in vacuum.

and they are respectively given by $OPL_C = |OR| + |RC|$ and $OPL_D = |OP| + n|PQ| + n|QD|$. Ray D emerges from point O and makes angle θ with x-axis. At point P, Snell's law can be applied to extract refraction angle (α) from the equation $\sin \theta = n \sin \alpha$. By equating optical paths, we obtain

$$q + nh = \sqrt{y_1^2 + q^2} + n\sqrt{(y - y_1)^2 + (x - q)^2} + n(h - y) \quad (3)$$

where y_1 is the distance $|PR|$ shown in Figure 1, namely $y_1 = q \tan \theta$. Also, for the line passing thorough points P and Q, we have the relation

$$y - y_1 = \tan \alpha (x - q) \quad (4)$$

Frankly speaking, it is difficult to find an explicit relation between x and y as in Equation 2 since both x and y are functions of the angle θ . However, one can obtain two parametric equations representing the surface 2. After doing some algebra, height of the ray at surface 2 can be found as:

$$y(\theta) = \frac{q(n^2 \sec \theta + 1 - \sec \theta)}{n^2 \operatorname{cosec} \theta - 1} \quad (5)$$

By using Equation 4, the abscissa can be evaluated from:

$$x(\theta) = q + \frac{y - q \tan \theta}{\tan(\arcsin[\sin(\theta)/n])} \quad (6)$$

In the manufacturing process, the center part of the lens is removed as a stairs shape to reduce weight and material cost as shown in Figure 2a. Of course, this change does not effect the illumination performance since the top surface of the lens (before detector) is nevertheless a plane. Finally, three-dimensional (3D) solid form of the lens is simply obtained by rotating the lens in y-axis as shown in Figure 2b.

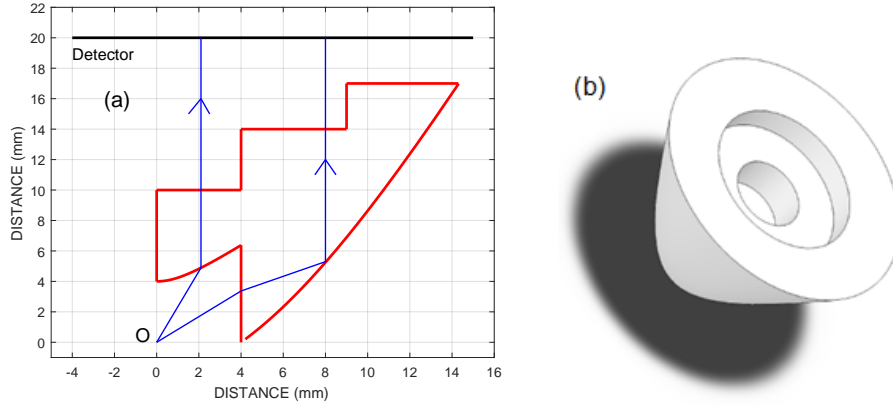


Fig. 2. Schematic diagram illustrating the surfaces of final lens for $p = q = 4$ mm, $h = 17$ mm and $n = 1.49$ (a) in 2D and (b) in 3D.

3. Optical Simulation

The equations derived for 2D free-form lens geometry and the point-like source are implemented in a Matlab programming language to attain initial calculations related to ray tracing for single wavelength. However, in practice one needs 3D geometry and LED which is neither a point-like nor a monochromatic source.

Fortunately, there are solid modeling softwares to obtain 3D geometry and assign desired polymeric material to the lens. Also, LED manufacturers distribute comprehensive ray-tracing data files to be used in optical simulations such as eulumdat, ray and spectrum files. In principle, LED is considered to be a point source in eulumdat file which is used for a quick analysis. Whereas, the ray file represents actual spatial and angular distribution of rays originating from the outer surface of LED. Therefore, ray files can be used in more realistic simulations. The spectral distribution of LED (wavelengths emitted and corresponding weights) are stored in spectrum files.

In this study, Zemax OpticStudio 20.1, which is very good at comprehensive ray tracing software, is used for the optical simulations. In Non-Sequential Mode of Zemax, one can include simulation files of LED, the 3D geometry of the lens and a suitable rectangular detector which is basically a counter of rays hitting on it. PMMA ($C_5H_8O_2$)_n material is assigned to the solid model of the lens since its transmittance for the visible and near infrared optical regions is greater than 90%.

Two types of LED provided by Osram Company [9] are chosen in simulations. They are SFH 4718A which is an IR LED whose peak irradiance is

at 850 nm and LUW H9GP a *white* LED having color temperature of 6500 K. 3D lens and IR LED used in this study are shown in Figure 3 for two different separation, d , between lens and LED. d is one of the important parameter in the design since it significantly affects the light distribution and number of photon hits on the detector. In this study, $d = 0.1$ mm is found to be optimum for both LED models.

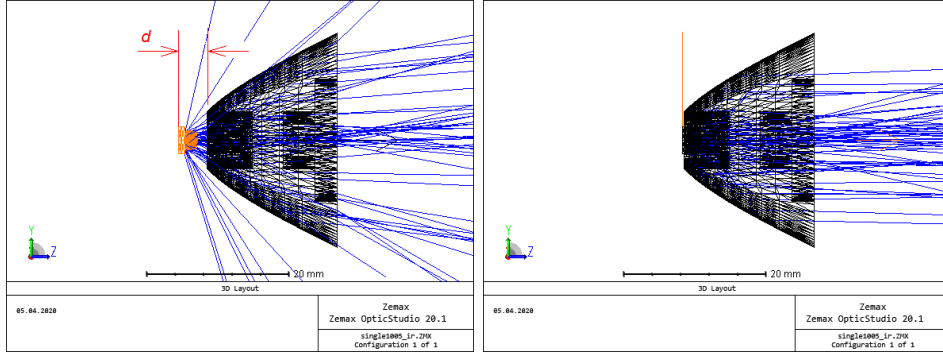


Fig. 3. The 3D lens and IR LED imported to Zemax. The rays in layouts are obtained from the LED's ray file. Left, LED is placed at $d = 4$ mm back of the lens. This little misalignment results in a wide angle ray distribution. Right, LED is placed its optimum position (at $d = 0.1$ mm) where the outgoing rays are almost parallel to $+z$ -axis defined from left to right in Zemax.

In the analyses, totally 5 million (both from eulumdat file and ray file) emitted from LEDs are used. For both models, spectrum files are also considered. Figure 4 shows spot diagrams obtained at a distance 100 m from LED and free-form lens system on the rectangular detector whose size is $15 \text{ m} \times 15 \text{ m}$. Luminous flux of white LED is selected as 100 lm and radiant power of the IR LED is fixed to 1 W. When using eulumdat files, as we expect, almost all of the rays fall on the detector and produce a very small light spot. However, the use of ray files result in relatively wider spot sizes at the same distance.

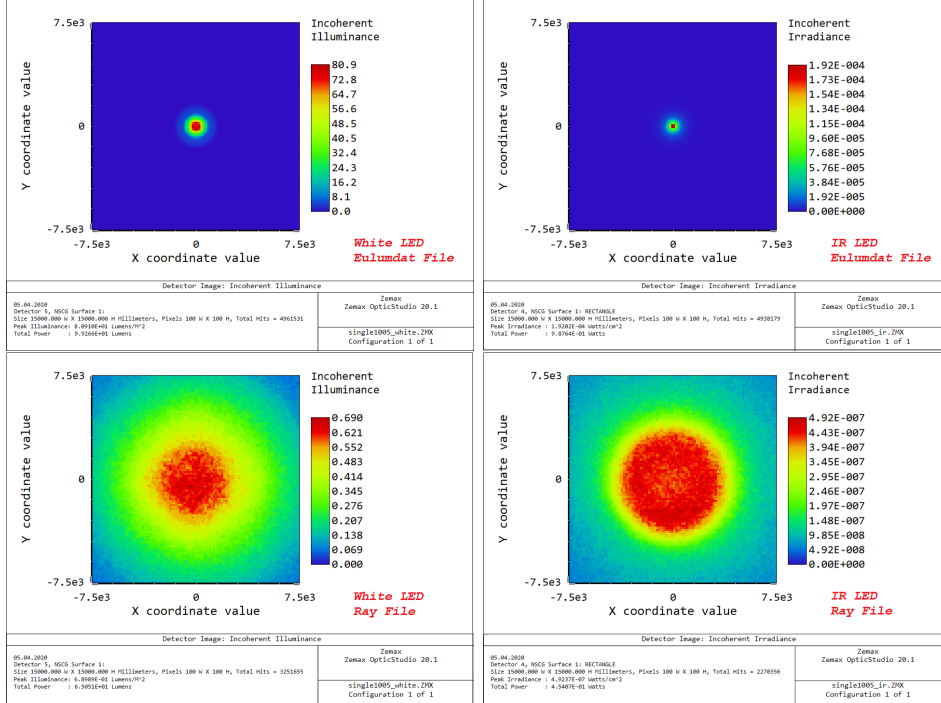


Fig. 4. Spot diagrams obtained on a rectangular detector being 100 m away from LED and lens system. Eulumdat, ray and spectrum files are used in ray tracing.

In addition, the study is repeated for two more polymers as well; PC (polycarbonate, $(C_{16}H_{14}O_3)_n$) and PS (polystyrene, $(C_8H_8)_n$). The simulation performance for three materials when using ray and spectrum files are summarized in Table 1. Obviously, PMMA exhibits the best performance in terms of total optical power on the detector. This is because the transmittance of the PMMA in visible and near IR region is greater than the others. On the other hand, one can obtain a smaller RMS spot size on the detector when using PC as a lens material.

Table 1. Simulation results obtained by using ray and spectrum files of LEDs for three polymeric materials. All values are calculated on $15\text{ m} \times 15\text{ m}$ detector at 100 m from the lens. Total source power of the LEDs are 100 lm and 1 W respectively. Total number of photon hits per total number of generated rays ($N = 1 \times 10^6$) on the detector are also given.

Quantity	LED	PMMA	PC	PS
RMS Spot diameter	White	2.5 m	2.4 m	2.6 m
Total luminous power	White	65.1 lm	57.7 lm	57.3 lm
Total hits / N	White	65.1 %	57.5 %	56.8 %
RMS Spot diameter	IR	3.0 m	2.3 m	2.8 m
Total radiant power	IR	0.45 W	0.36 W	0.35 W
Total hits / N	IR	45.5 %	35.5 %	34.7 %

4. Manufacturing the Free-Form Lens and Building Projector

Manufacturers prefers mostly PMMA as a lens material since it has lower index of refraction and better optical transparency properties [8]. Therefore, a prototype of the proposed lens is manufactured by using PMMA via plastic injection molding method. Figure 5a shows the fabricated free-form lens for $p = q = 4\text{ mm}$, $h = 20\text{ mm}$ and $n = 1.49^2$. In addition, two prototype projectors are built by combining nine lenses in the form of a 3×3 array as shown in Figure 5b.

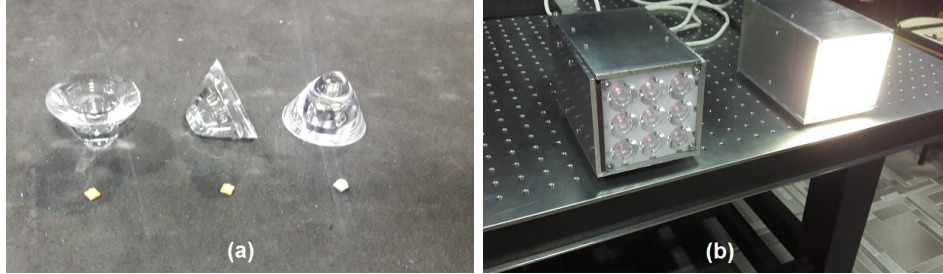


Fig. 5. (a) Fabricated lenses made from PMMA and LEDs used in the study. (b) Two projectors built from the these lenses when low electrical powers are supplied.

5. Optical Performance of Projectors

In order to test the optical performance of the projector, two measurements are carried out using IR LEDs (Osram SFH 4718A) and white LEDs (Osram LUW H9GP). In the measurements, both projectors are supplied

² This is the average refractive index of PMMA for the wavelength range from 400 nm to 1000 nm .

by an LED driver whose maximum electrical power is about 7.7 W ($V = 20\text{-}22$ V and $I = 0.35$ A).

The simulation and experimental results for the angular light distributions are shown in Figure 6. It is obvious that the experimental data (solid red lines) are almost consistent with the simulations (solid blue lines). Full width half maximum (FWHM) values of the distributions are approximately evaluated as 7.0° for white light projector, and 9.3° for IR projector. However, $FWHM \approx 6.1^\circ$ for IR projector in the simulation. Apparently, both projectors can be used for long range (or narrow angle) illumination.

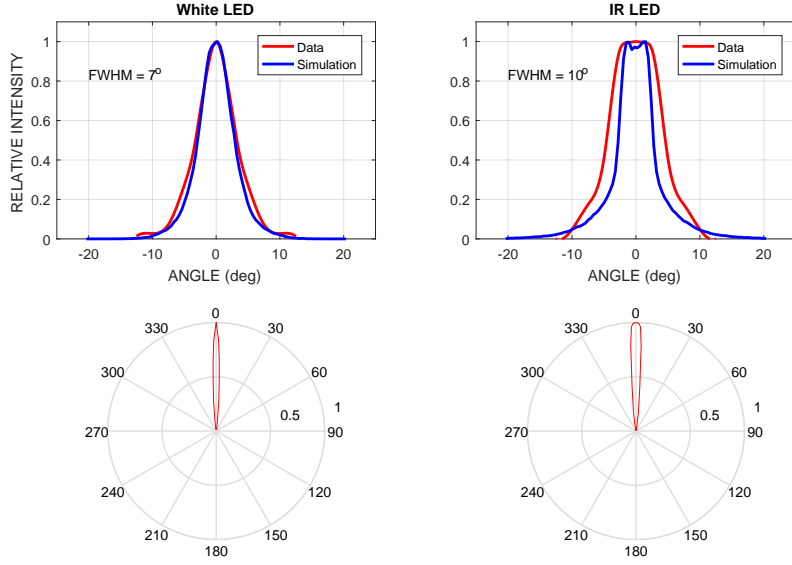


Fig. 6. Comparison of goniophotometric measurements with simulations in both cartesian and polar coordinates.

Second measurements are performed to test the dependence of light intensity as a function of distance. In the IR region at around 850 nm, optical powers are measured by using Newport 843-R Powermeter. The counterpart study is repeated for the white light projector. In this case, illuminance data are acquired by means of Testo 435 Luxmeter. Measurements are made at various distances as shown in Figure 7. The experimental data and simulation results are represented by red stars and by solid blue lines respectively. Measured values are less than that of simulation as we expect. This is possible because the manufactured prototype projectors have some misalignments, however, simulations represent the perfect geometry

and alignment.

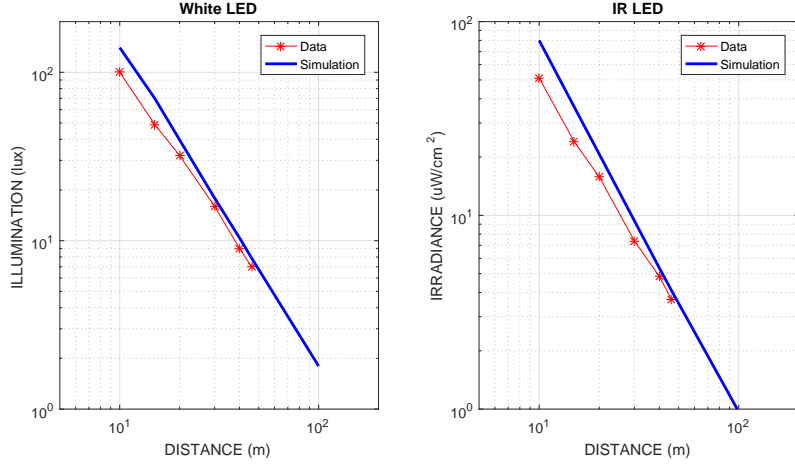


Fig. 7. Simulation and measurement results of peak illuminance (left) and peak irradiance (right) as a function of distance from projectors.

Finally, the illumination performance of projectors are shown in Figure 8. Two photographs of a 50 m long and dark corridor are taken after illumination³. The man at the end of corridor is seen clearly after illumination.



Fig. 8. Two photographs of a 50 m long and completely dark corridor taken by a webcam after illuminating by the projector with white LED (left) and with IR LED (right).

³ These photograph are taken by a webcam whose IR filter is removed so that full IR waves can also be seen as in Figure 8 (right).

6. Summary and Conclusion

In this study, a prototype of a free-form lens which can be used for long range illumination is designed and manufactured. Surfaces of the free-form lens are extracted by equating the optical path length of the rays from a point-like light source. Ray tracing simulations are performed in Zemax OpticStudio 20.1 where IR and visible LEDs are selected as light sources and various optical polymers (PMMA, PC and PS) are concerned as lens material.

In manufacturing of the lens PMMA is selected since it exhibits the best performance in terms of optical power calculated on the detector according to simulation results. Manufacturing is fulfilled by well known technique called the plastic injection molding method. Two LED projector prototypes containing nine lenses are built for visible illumination and IR irradiation applications. The optical measurements of these projectors are found to be consistent with simulations.

Finally, authors suggest that a larger array of such free-form lenses can be used as a LED projector for the purpose of long range illumination since its angular divergence is less than 10° and it requires low electric power. These projectors may be useful in optical wireless communication, in illumination of car parks or stadiums, in headlights of vehicles and in houses or homesteads for the security purposes.

7. Acknowledgement

We wish to thank to the Scientific and Technological Research Council of Turkey (Türkiye Bilimsel ve Teknolojik Araştırma Kurumu, TÜBİTAK) for supporting us to manufacture the proposed free-form lens and the projector.

REFERENCES

- [1] H. Ries and J. Muschaweck, *Opt. Soc. Am. A*, 19 (2002)
- [2] Y. Ding et al, *Opt. Soc. Am. A*, 16 (2008) 12958-12966
- [3] B. Yang et al, *Optik*, 120 (2009) 74-78
- [4] N.D.Q. Anh et al, *Opt. Soc. Am.*, 53 (2014)
- [5] S. Hu et al, *Appl. Opt.*, 54 (2015) 9990-9999
- [6] R.J. Lin and C.C Sun, *Optical Engineering*, 55 (2016)
- [7] Zemax OpticStudio, Version Oct 28 2019 <https://www.zemax.com>
- [8] N. Sultanova et al, *Acta Physica Polonica A*, 116 (2009)
- [9] Osram, <https://www.osram.com>, (2020)